International Endodontic Journal

doi:10.1111/j.1365-2591.2012.02083.x

Bioactivity of EndoSequence Root Repair Material and Bioaggregate

N. Shokouhinejad[1,2,3], M. H. Nekoofar[1,2,4], H. Razmi[1,2], S. Sajadi[1], T. E. Davies[5], M. A. Saghiri[6], H. Gorjestani[7] & P. M. H. Dummer[4]

[1]Dental Research Center, Tehran University of Medical Sciences, Tehran; [2]Department of Endodontics, School of Dentistry, Tehran University of Medical Sciences, Tehran; [3]Iranian Center for Endodontic Research, Tehran; Iran; [4]Endodontology Research Group, School of Dentistry, Cardiff University, Cardiff; [5]School of Chemistry, Cardiff University, Cardiff; UK; and [6]Department of Dental Material, Dental School, Azad University/Kamal Asgar Research Center (KARC), Tehran; and [7]Oral and Dental Diseases Research Center, School of Dentistry, Kerman University of Medical Sciences, Kerman; Iran

Abstract

Shokouhinejad N, Nekoofar MH, Razmi H, Sajadi S, Davies TE, Saghiri MA, Gorjestani H, Dummer PMH. Bioactivity of EndoSequence Root Repair Material and Bioaggregate. *International Endodontic Journal*, **45**, 1127–1134, 2012.

Aim To evaluate the bioactivity of Bioaggregate (BA), EndoSequence Root Repair Material (ERRM), and white ProRoot Mineral trioxide aggregate (MTA).

Methodology Sixty horizontal root sections with standardized canal spaces were divided randomly into 3 groups ($n = 20$) and filled with white ProRoot MTA (groups 1 and 2), BA (groups 3 and 4) or ERRM putty (groups 5 and 6). The specimens of groups 1, 3 and 5 (each of 10) were immersed in phosphate-buffered saline (PBS) for 1 week and those of groups 2, 4 and 6 (each of 10) for 2 months. After the experimental periods, the specimens were processed for scanning electron microscopy (SEM) observations. Precipitation of apatite crystals on the surfaces of the cements and/or at the dentine–cement interface was evaluated and analysed elementally by energy dispersive X-ray (EDX) instrument.

Results Analysis of specimens revealed various surface morphologies that were dependent on the material and immersion time in PBS. The formation of precipitates was observed on the surfaces of all materials at 1 week, which increased substantially over time. After 2 months, the surface of the cements was changed dramatically and consisted of a substantially greater amount of apatite aggregates. Interfacial layers in some areas of the dentine–cement interface were found only following 2 months of immersion. Precipitates on MTA revealed high peaks of Ca, Si and O after 1 week of immersion; after 2 months, high peaks of Ca, P and O were present. Precipitates on BA and ERRM displayed high Ca, P O peaks after both 1 week and 2 months.

Conclusion Exposure of MTA, BA and ERRM to PBS resulted in precipitation of apatite crystalline structures that increased over time. This suggests that the tested materials are bioactive.

Keywords: apatite, bioactivity, bioaggregate, bioceramic materials, EndoSequence Root Repair Material, mineral trioxide aggregate.

Received 26 February 2012; accepted 4 May 2012

Introduction

Mineral trioxide aggregate (MTA), a bioceramic aggregate (Alanezi *et al.* 2010) with several clinical applications, has gained widespread use (Torabinejad & Chivian 1999, Felippe *et al.* 2006). Recently, new

Correspondence: Dr. Mohammad H. Nekoofar, Endodontology Research Group, School of Dentistry, Cardiff University, Heath Park, Cardiff, CF14 4XY, UK (e-mail: nekoofar@yahoo.com, nekoofarmh@cardiff.ac.uk)

bioceramic materials have been introduced as alternatives to MTA (Lovato & Sedgley 2011). Bioaggregate (BA) (Innovative BioCeramix, Vancouver, BC, Canada) is a bioceramic material delivered as powder of nanoparticles composed of tricalcium silicate, dicalcium silicate, calcium phosphate monobasic, amorphous silicon dioxide and tantalum pentoxide (Zhang *et al.* 2009). Its constitution is similar to white MTA, differing mostly by being aluminium free (De-Deus *et al.* 2009) and containing calcium phosphate monobasic and tantalum pentoxide. The latter was added as a radiopacifier in place of the bismuth oxide in MTA (Zhang *et al.* 2009, Park *et al.* 2010). Studies have demonstrated a comparable antibacterial effects (Zhang *et al.* 2009), biocompatibility (De-Deus *et al.* 2009) and sealing ability (Leal *et al.* 2011) of BA to those of MTA. It has been reported that BA induced mineralized tissue formation (Yuan *et al.* 2010) and differentiation of human PDL fibroblasts (Yan *et al.* 2010).

EndoSequence Root Repair Material (ERRM) (Brasseler USA, Savannah, GA, USA) is another bioceramic material that has been developed recently (Damas *et al.* 2011). According to the manufacturer, ERRM is composed of calcium silicates, zirconium oxide, tantalum oxide, calcium phosphate monobasic and filler agents. It is produced as a premixed product in both mouldable putty and preloaded syringeable paste to provide the clinician with a homogeneous and consistent material that sets in the presence of moisture. ERRM has been demonstrated to be biocompatible (Alanezi *et al.* 2010, Ma *et al.* 2011), antibacterial (Lovato & Sedgley 2011) and be able to seal root-end cavities (Nair *et al.* 2011).

A bioactive material is able to interact with living tissues, resulting in the formation of an apatite layer, biomineralization, at the material-tissue interface (Hench & Wilson 1984, Kokubo & Takadama 2006). Evaluation of apatite formation on the surface of a material when exposed to a simulated body fluid is an approved method to examine *in vivo* hard tissue bioactivity (Kokubo & Takadama 2006). Formation of hydroxyapatite or carbonated apatite as a result of the interaction between MTA and phosphate-containing fluids suggesting its bioactivity has been reported (Sarkar *et al.* 2005, Bozeman *et al.* 2006, Tay *et al.* 2007, Reyes-Carmona *et al.* 2009, Gandolfi *et al.* 2010a,b,c). However, there is little information available on the bioactivity of BA and ERRM. This study aimed to evaluate the bioactivity of BA, ERRM, and white ProRoot MTA (Dentsply Tulsa Dental, Tulsa, OK, USA) following 1-week and 2-month immersion in phosphate-buffered saline (PBS).

Materials and methods

Thirty extracted single-rooted human teeth were collected. After removing the crowns, the middle portion of each root was sectioned transversely using a water-cooled diamond saw on a precision cut-off machine (Mecatome, Presi, France) to obtain two 2.00 ± 0.05-mm-thick root sections. The lumen of the each section was enlarged with size 2–5 Gates Glidden burs (Dentsply Maillefer, Ballaigues, Switzerland) to obtain a standardized diameter of 1.3 mm. The specimens were immersed in 17% EDTA for 3 min followed by 5.25% NaOCl and then washed with distilled water. The root sections were randomly divided into six groups each of 10 as follows:

Groups 1 and 2: An aliquot of 0.33 mL distilled water was mixed with 1 g of white ProRoot MTA powder (Nekoofar *et al.* 2007) and the resultant slurry placed in the canal space of each root section with minimal pressure.

Groups 3 and 4: An aliquot of 0.33 mL deionized water provided by the manufacturer was mixed with the entire increment of BA powder inside the sachet (1 g). The resultant slurry was then introduced into the canal space with minimal pressure.

Groups 5 and 6: The canal spaces were filled with the premixed ERRM putty.

After that, specimens were wrapped in pieces of gauze soaked in PBS for 1 h and the root sections were then immersed individually in 2 mL of PBS solution (pH = 7.2) within sterile Eppendorf plastic tubes (Eppendorf-Elkay, Shrewsbury, MA, USA). In groups 1, 3 and 5, the root sections were stored in PBS for 1 week and in groups 2, 4 and 6 for 2 months. The PBS solution was renewed weekly. All specimens were incubated at 37 °C.

Cement surface and cement-dentine interface SEM-EDX analyses

After the experimental periods, the root sections were dried at 37 °C for 24 h. Specimens were then mounted on metallic stubs, gold sputtered and examined under a scanning electron microscope equipped with an energy dispersive X-ray instrument (SEM-EDX) (Vega II XMU, Tescan, Czech Republic) at an accelerating voltage of 15 kV. SEM photomicrographs at several magnifications (×30–25 000) were taken to identify the formation of precipitates on the surface of cements and/or at the dentine–cement interfaces. The ultrastructure of the precipitates and interfacial layers was analysed with SEM, and their elemental composition was determined using EDX.

Results

SEM analysis

Scanning electron microscopy analysis revealed limited precipitate formation on the surfaces of all three cements after 1 week of immersion in PBS (Fig. 1a). None of the specimens were associated with precipitates at the dentine–cement interface following 1 week.

After 2 months, the topography of the cements was dramatically changed and their surfaces were covered by a substantially greater amount of precipitate (Fig. 1b). All 2-month specimens were associated with an interfacial layer between the materials and dentine in several areas (Fig. 1c,d).

Analysis of specimens revealed various surface morphologies dependent on the material and immersion time in PBS. Photomicrographs of MTA specimens after 1 week showed the presence of crystalline phases with two distinct morphologies: agglomerates of large faceted particles and aggregates of smaller submicron particles (Fig. 2a). After 2 months, SEM analysis of precipitates revealed the particle morphology to be more uniform than after 1 week for MTA specimens. At higher magnifications, spherical aggregates composed of smaller particles (Fig. 2c) as well as network of acicular crystals were observed (Fig. 2d).

Scanning electron microscopy evaluation of BA after 1 week of immersion revealed a uniform and homogeneous layer with no individual particles of micron size (Fig. 3a). After 2 months, BA specimens had spherical precipitates (Fig. 3c). Spherical aggregates composed of minute particles around the periphery were also seen, similar to those observed for MTA after 2 months.

EndoSequence Root Repair Material immersed in PBS for 1 week displayed smooth aggregates composed of individual and fused globular particles (Fig. 4a). After 2 months of immersion, the ERRM specimens had substantial crystal growth out of the plane of the material. Analysis at higher magnification revealed the precipitates to be clusters of spherical acicular particles (Fig. 4c).

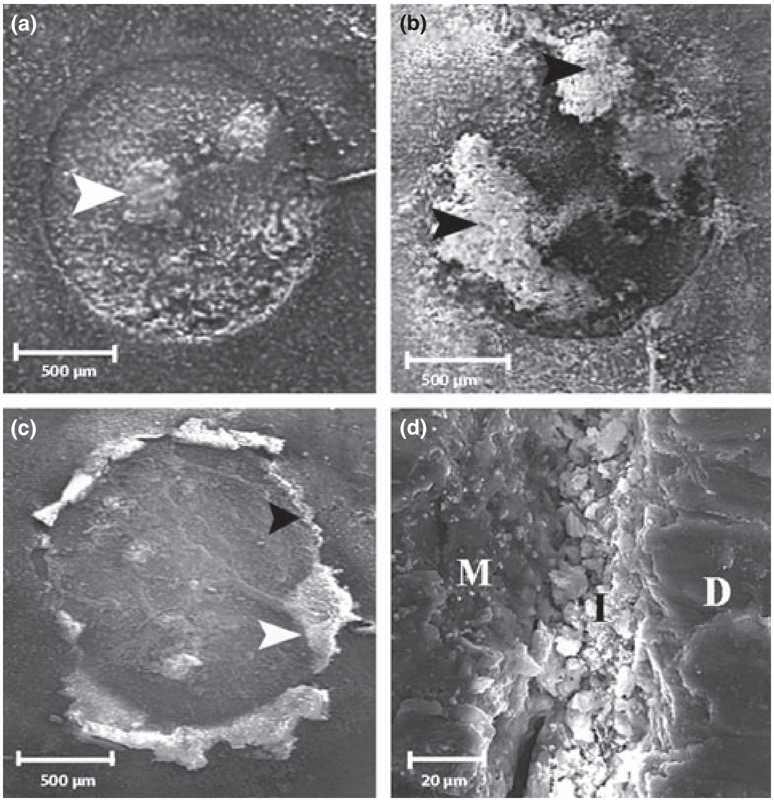

Figure 1 Scanning electron microscopy examination of specimens immersed in phosphate-buffered saline (PBS) for 1 week and 2 months. A specimen immersed in PBS for 1 week demonstrating formation of precipitates (white arrowhead) on the surface of material (a). A 2-month specimen shows a large amount of precipitates (black arrowheads) (b). Formation of precipitates at the dentine–material interface (black arrowhead) extending over material and dentine surfaces (white arrowhead) in some areas following 2 months of immersion (c). At higher magnification, formation of an interfacial layer is seen at the material-dentine interface (d). M, material; I, interface; D, dentine.

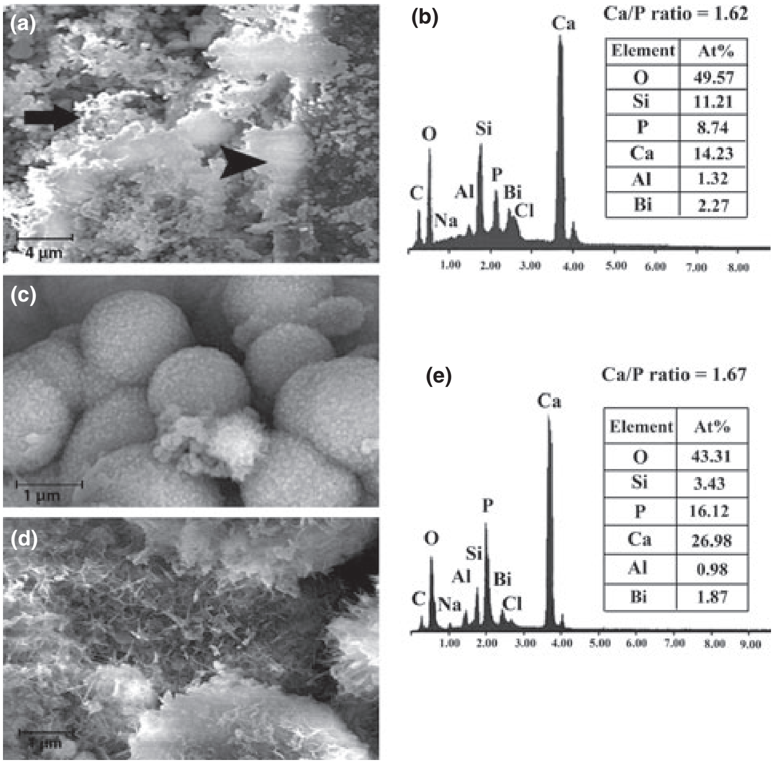

Figure 2 SEM-EDX analyses of Mineral trioxide aggregate (MTA). Photomicrograph of a specimen immersed in phosphate-buffered saline for 1 week showing agglomerates of large faceted (black arrowhead) particles and aggregates of smaller submicron particles (black arrow) (a). Energy dispersive X-ray (EDX) analysis of precipitates formed on MTA after 1 week revealed high Ca, Si and O peaks (b). A specimen immersed for 2 months demonstrating spherical aggregates composed of minute particles along the periphery (c) and acicular crystals creating network-like aggregates (d). EDX analysis of 2-month precipitates showed high Ca, P and O peaks (e). Semiquantitative chemical composition of precipitates and Ca/P ratio can be seen (b, e).

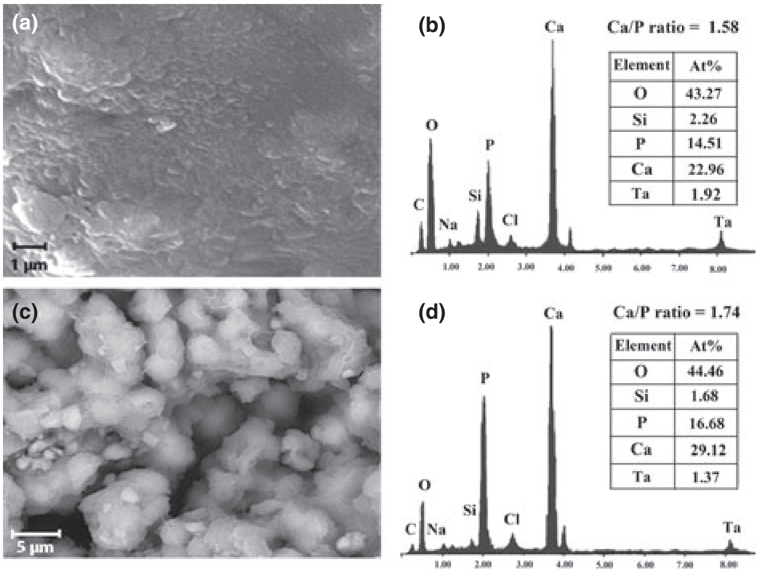

Figure 3 SEM-EDX analyses of BA. Micrograph of a 1-week specimen showing a homogeneous layer with no individual particles of micron size (a). After 2 months, BA showed spherical precipitates (c). Energy dispersive X-ray (EDX) on precipitates over BA showed no difference after 1 week (b) and 2 months (d) and displayed high Ca, P and O peaks. EDX revealed the presence of Ta and absence of Bi and Al. Semiquantitative chemical composition of precipitates as well as Ca/P ratio can be seen (b, d).

EDX analysis

Analysis of the elemental composition of precipitates formed on the cements surface in all materials displayed high peaks of Ca. In addition, the presence of C, Na and Cl was also revealed.

After 1 week, precipitates on MTA had high peaks of Ca, Si and O (Fig. 2b) and after 2 months high peaks of Ca, P and O. Peaks of Bi and Al were also discovered.

Precipitates on BA displayed high Ca, P and O peaks after 1 week (Fig. 3b) and 2 months (Fig. 3d)

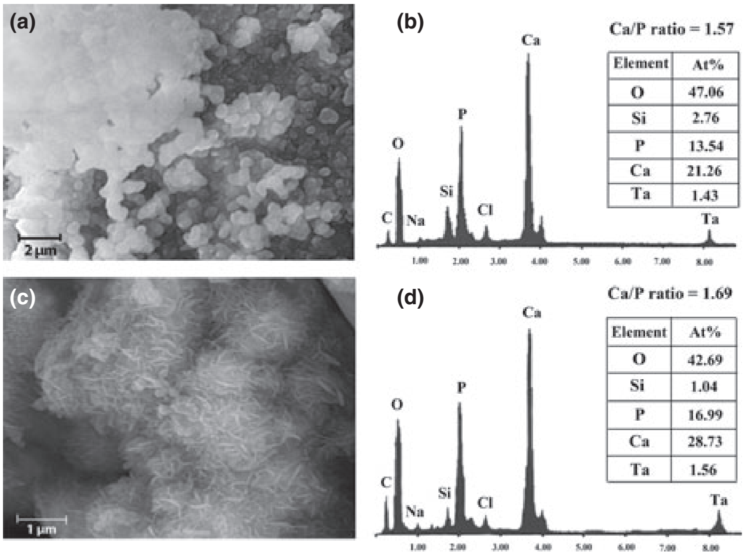

Element	At%
O	47.06
Si	2.76
P	13.54
Ca	21.26
Ta	1.43

Element	At%
O	42.69
Si	1.04
P	16.99
Ca	28.73
Ta	1.56

Figure 4 SEM-EDX analyses of ERRM. Image of the surface of a 1-week ERRM specimen showing smooth aggregates composed of individual and fused globular particles (a). After 2 months, precipitates on the ERRM showed to be clusters of spherical acicular particles (c). No marked difference was found between the elemental composition of precipitates on ERRM formed at 1 week (b) and 2 months (d) which showed high Ca, P and O peaks. The presence of Ta and absence of Bi and Al were displayed. Semiquantitative chemical composition as well as Ca/P ratio of precipitates can be seen (b, d).

with no noticeable difference. Compared with MTA, the absence of Bi and Al and the presence of Ta were obvious.

The precipitates on ERRM contained mainly Ca, P and O and showed no notable difference between 1 week (Fig. 4b) and 2 months (Fig. 4d). In contrast to MTA and similar to BA, precipitates formed over ERRM had no Bi and Al but did contain Ta.

Semiquantitative chemical composition of precipitates demonstrated in Figs 2b, 2e, 3b, 3d, 4b and 4d showed different values of Ca/P ratios depending on the analysed area and immersion time. Ca/P ratios observed in specimens immersed in PBS for 1 week were 1.5–1.62 and for 2-month specimens were 1.67–1.75. There was an increase in Ca/P ratios with increasing immersion time.

Energy dispersive X-ray instrument analysis of the newly formed distinct layers that precipitated at dentine–cements interfaces of the 2-month specimens revealed that the composition of the interfacial layer was the same as that of the precipitates formed on the cements surface following 2 months of immersion in PBS.

Discussion

In this study, the bioactivity of various bioceramic materials including BA, ERRM and MTA was evaluated by exposure of root sections containing the materials in standard canal lumens to PBS, a recommended method for the evaluation of hard tissue bioactivity (Kokubo & Takadama 2006). The findings revealed the formation of apatite precipitates on the surface of the materials following 1 week of immersion in PBS, which increased substantially over time. This is in accordance with the findings of others (Sarkar *et al.* 2005, Bozeman *et al.* 2006, Tay *et al.* 2007, Reyes-Carmona *et al.* 2009) who concluded that the interaction of MTA with a phosphate-containing solution resulted in the formation of apatite crystals.

The precipitation of apatite appears to begin within the first hours of immersion in PBS (Reyes-Carmona *et al.* 2009). In addition, according to Gandolfi *et al.* (2010a,b,c), increasing the immersion time in simulated tissue fluid enhanced the precipitation of apatite crystals. Calcium ions released by MTA react with phosphate in PBS, a calcium-free but phosphate-rich solution, resulting in the formation of hydroxyapatite (Sarkar *et al.* 2005, Bozeman *et al.* 2006) or carbonated apatite (Tay *et al.* 2007, Reyes-Carmona *et al.* 2009, Gandolfi *et al.* 2010b). The latter represent the mineral phase of hard tissues (Tay *et al.* 2007).

Although the precipitation was observed on the cement surfaces following 1 week of immersion, the formation of an interfacial layer at the dentine–cements junction was found only at 2 months. Previous studies also revealed that the interaction of MTA with dentine after exposure to PBS for 2 months resulted in formation of interfacial layers (Sarkar *et al.* 2005, Reyes-Carmona *et al.* 2009, 2010a,b). Gandolfi *et al.* (2010a) demonstrated that curing of calcium silicate cements in PBS affected the size of aggregated crystals as well as morphology and chemical composition of cement surface.

Immediately following the hydration of MTA powder, Ca and OH ions are released from tricalcium and/or dicalcium silicate into the surrounding environment resulting in the formation of a calcium hydroxide (portlandite) precipitate and calcium silicate hydrate (CSH) gel (Camilleri 2007). Over time, in the presence of phosphorus ions included in phosphate-containing media, greater precipitations occurs (Gandolfi *et al.* 2010a). In this study, the same trend was observed with larger crystalline apatite structures being observed when the immersion time increased.

Depending on the materials and immersion time, SEM analysis of specimens revealed different surface morphologies. After the first week, the surface morphology varied between the materials. For example, MTA was associated with agglomerates of large faceted and smaller submicron particles. In contrast, BA displayed a uniform and homogeneous surface. This finding is in accordance with that of Hashem & Wanees Amin (2012) who reported irregular and hexagonal crystals with MTA, but the absence of large crystals with BA after a short immersion time in PBS.

In this study, ERRM displayed a different surface morphology compared with BA and MTA after 1 week. Smaller individual particles distributed throughout the amorphous matrix were observed following immersion of ERRM in PBS. Varying surface topographies of the materials might be attributed to their constituents and form of delivery. BA and ERRM are composed of calcium phosphate and calcium silicates whilst MTA lacks calcium phosphate in its composition. Moreover, because of the putty delivery form of ERRM, it includes fillers and thickening agents that may impact on its hydration.

By increasing the immersion time in PBS, the surface topography of the materials changed dramatically. All materials had mature apatite agglomerates on their surfaces. Furthermore, formation of apatite crystalline structures at the dentine–material interface of all cements was found following 2 months of immersion. MTA samples immersed for 2 months had spherical precipitates composed of smaller particles and aggregates of acicular crystallites. Formation of spherical precipitates with apatite clusters or acicular crystallites along the periphery after immersion of MTA in PBS for 2 months has also been demonstrated (Sarkar *et al.* 2005, Reyes-Carmona *et al.* 2009). BA and ERRM were also associated with mature apatite-like of spherical aggregates on their surfaces and/or at dentine–material interfaces at 2 months.

Elemental analysis revealed the precipitates formed on the surfaces of MTA at 2 months and BA and ERRM at both immersion times were composed mainly of Ca, P and O. The low peak of P in MTA specimens after 1 week could be ascribed to the absence of phosphorus in ProRoot MTA, which has been reported in several studies (Asgary *et al.* 2004, 2006, Camilleri *et al.* 2005, Gandolfi *et al.* 2010b) as well as the limited exposure time of the material to PBS. High P peaks detected in precipitates formed on BA and ERRM after 1 week but not on MTA specimens could be explained by the presence of calcium phosphate in BA and ERRM.

In this study, the high peaks of Ca and P after 2 months of immersion in PBS are consistent with other studies. This demonstrates the bioactivity of MTA and MTA-like cements via the formation of hydroxyapatite or carbonated apatite, composed mainly of Ca and P, following increasing the immersion times in phosphate-containing fluids (Sarkar *et al.* 2005, Reyes-Carmona *et al.* 2009, Gandolfi *et al.* 2010a,b,c).

In this study, the Ca/P ratio of the precipitates increased with increased immersion time. The Ca/P ratios were 1.5–1.62 following 1 week of immersion in PBS that increased to 1.67–1.75 following 2 months. The formation of carbonated apatite has been stated to be a two-stage process that correlates to increased Ca/P ratios (Tay *et al.* 2007).

EDX on MTA specimens revealed peaks of Al and Bi. In contrast, BA and ERRM were free of aluminium. However, Camilleri (2008) stated that the presence of aluminium was scarce. Both BA and ERRM showed a tantalum peak. These findings are in agreement with Park *et al.* (2010) who concluded that BA contained tantalum oxide instead of bismuth oxide as a radiopacifier and lacked Al in its constituents compared with white ProRoot MTA.

The high peak of O observed in all of the specimens is attributed to the presence of water (Gandolfi *et al.* 2010c). The presence of C might also be related to the presence of a calcium carbonate precipitate, which is formed by the reaction of Ca and environmental carbonate ions (Gandolfi *et al.* 2010b). Furthermore, detection of Na and Cl is linked to the PBS (Gandolfi *et al.* 2010c).

In this study, acicular crystalline structures were observed in aggregates formed over MTA and ERRM after 2 months of immersion in PBS. According to Camilleri (2008), Gandolfi *et al.* (2010d) and Nekoofar *et al.* (2011), following the initiation of the hydration process of MTA, needle-like crystals of ettringite (hydrated calcium–aluminium–sulphate) are formed as a result of a reaction between gypsum and calcium aluminate hydrate. In the absence of the aluminate phase in aluminium free materials, the lack of ettringite crystals can be anticipated. As EDX also displayed Ca and P peaks, but not Al and S, in the composition of the acicular deposits formed on BA and ERRM, it seems they were apatite-like aggregates that formed following the longer immersion in phosphate-containing solution and thus different from the needle-like crystals of ettringite. By increasing the immersion time, the alteration in morphology of apatite crystals can be explained by precipitation and dissolution of various elements at the superficial layers (Reyes-Carmona *et al.* 2009).

Conclusion

Exposure of MTA, BA and ERRM to simulated tissue fluid, PBS, resulted in precipitation of apatite crystals that became larger with increasing immersion times. It can be concluded that all of the bioceramic materials in this study are bioactive.

Acknowledgement

This study was part of a M.S. thesis supported by Tehran University of Medical Sciences (grant no: 14217).

References

Alanezi AZ, Jiang J, Safavi KE, Spangberg LS, Zhu Q (2010) Cytotoxicity evaluation of endosequence root repair material. *Oral Surgery, Oral Medicine, Oral Pathology, Oral Radiology, and Endodontology* **109**, e122–5.

Asgary S, Parirokh M, Eghbal MJ, Brink F (2004) A comparative study of white mineral trioxide aggregate and white Portland cements using X-ray microanalysis. *Australian Endodontic Journal* **30**, 89–92.

Asgary S, Parirokh M, Eghbal MJ, Stowe S, Brink F (2006) A qualitative X-ray analysis of white and grey mineral trioxide aggregate using compositional imaging. *Journal of Materials Science. Materials in Medicine* **17**, 187–91.

Bozeman TB, Lemon RR, Eleazer PD (2006) Elemental analysis of crystal precipitate from gray and white MTA. *Journal of Endodontics* **32**, 425–8.

Camilleri J (2007) Hydration mechanisms of mineral trioxide aggregate. *International Endodontic Journal* **40**, 462–70.

Camilleri J (2008) Characterization of hydration products of mineral trioxide aggregate. *International Endodontic Journal* **41**, 408–17.

Camilleri J, Montesin FE, Di Silvio L, Pitt Ford TR (2005) The chemical constitution and biocompatibility of accelerated Portland cement for endodontic use. *International Endodontic Journal* **38**, 834–42.

Damas BA, Wheater MA, Bringas JS, Hoen MM (2011) Cytotoxicity comparison of mineral trioxide aggregates and EndoSequence bioceramic root repair materials. *Journal of Endodontics* **37**, 372–5.

De-Deus G, Canabarro A, Alves G, Linhares A, Senne MI, Granjeiro JM (2009) Optimal cytocompatibility of a bioceramic nanoparticulate cement in primary human mesenchymal cells. *Journal of Endodontics* **35**, 1387–90.

Felippe WT, Felippe MC, Rocha MJ (2006) The effect of mineral trioxide aggregate on the apexification and periapical healing of teeth with incomplete root formation. *International Endodontic Journal* **39**, 2–9.

Gandolfi MG, Ciapetti G, Taddei P *et al.* (2010a) Apatite formation on bioactive calcium-silicate cements for dentistry affects surface topography and human marrow stromal cells proliferation. *Dental Materials* **26**, 974–92.

Gandolfi MG, Taddei P, Tinti A, De Stefano Dorigo E, Rossi PL, Prati C (2010b) Kinetics of apatite formation on a calcium-silicate cement for root-end filling during ageing in physiological-like phosphate solutions. *Clinical Oral Investigations* **14**, 659–68.

Gandolfi MG, Taddei P, Tinti A, Prati C (2010c) Apatite-forming ability (bioactivity) of ProRoot MTA. *International Endodontic Journal* **43**, 917–29.

Gandolfi MG, Van Landuyt K, Taddei P, Modena E, Van Meerbeek B, Prati C (2010d) Environmental scanning electron microscopy connected with energy dispersive x-ray analysis and Raman techniques to study ProRoot mineral trioxide aggregate and calcium silicate cements in wet conditions and in real time. *Journal of Endodontics* **36**, 851–7.

Hashem AA, Wanees Amin SA (2012) The effect of acidity on dislodgment resistance of mineral trioxide aggregate and bioaggregate in furcation perforations: an in vitro comparative study. *Journal of Endodontics* **38**, 245–9.

Hench LL, Wilson J (1984) Surface-active biomaterials. *Science* **226**, 630–6.

Kokubo T, Takadama H (2006) How useful is SBF in predicting in vivo bone bioactivity? *Biomaterials* **27**, 2907–15.

Leal F, De-Deus G, Brandao C, Luna AS, Fidel SR, Souza EM (2011) Comparison of the root-end seal provided by bioceramic repair cements and White MTA. *International Endodontic Journal* **44**, 662–8.

Lovato KF, Sedgley CM (2011) Antibacterial activity of endosequence root repair material and proroot MTA against clinical isolates of Enterococcus faecalis. *Journal of Endodontics* **37**, 1542–6.

Ma J, Shen Y, Stojicic S, Haapasalo M (2011) Biocompatibility of two novel root repair materials. *Journal of Endodontics* **37**, 793–8.

Nair U, Ghattas S, Saber M, Natera M, Walker C, Pileggi R (2011) A comparative evaluation of the sealing ability of 2 root-end filling materials: an in vitro leakage study using Enterococcus faecalis. *Oral Surgery, Oral Medicine, Oral Pathology, Oral Radiology, and Endodontology* **112**, e74–7.

Nekoofar MH, Adusei G, Sheykhrezae MS, Hayes SJ, Bryant ST, Dummer PM (2007) The effect of condensation pressure on selected physical properties of mineral trioxide aggregate. *International Endodontic Journal* **40**, 453–61.

Nekoofar MH, Davies TE, Stone D, Basturk FB, Dummer PM (2011) Microstructure and chemical analysis of blood-contaminated mineral trioxide aggregate. *International Endodontic Journal* **44**, 1011–8.

Park JW, Hong SH, Kim JH, Lee SJ, Shin SJ (2010) X-Ray diffraction analysis of white ProRoot MTA and Diadent BioAggregate. *Oral Surgery, Oral Medicine, Oral Pathology, Oral Radiology, and Endodontology* **109**, 155–8.

Reyes-Carmona JF, Felippe MS, Felippe WT (2009) Biomineralization ability and interaction of mineral trioxide aggregate and white portland cement with dentin in a phosphate-containing fluid. *Journal of Endodontics* **35**, 731–6.

Reyes-Carmona JF, Felippe MS, Felippe WT (2010a) The biomineralization ability of mineral trioxide aggregate and Portland cement on dentin enhances the push-out strength. *Journal of Endodontics* **36**, 286–91.

Reyes-Carmona JF, Felippe MS, Felippe WT (2010b) A phosphate-buffered saline intracanal dressing improves the biomineralization ability of mineral trioxide aggregate apical plugs. *Journal of Endodontics* **36**, 1648–52.

Sarkar NK, Caicedo R, Ritwik P, Moiseyeva R, Kawashima I (2005) Physicochemical basis of the biologic properties of mineral trioxide aggregate. *Journal of Endodontics* **31**, 97–100.

Tay FR, Pashley DH, Rueggeberg FA, Loushine RJ, Weller RN (2007) Calcium phosphate phase transformation produced by the interaction of the portland cement component of white mineral trioxide aggregate with a phosphate-containing fluid. *Journal of Endodontics* **33**, 1347–51.

Torabinejad M, Chivian N (1999) Clinical applications of mineral trioxide aggregate. *Journal of Endodontics* **25**, 197–205.

Yan P, Yuan Z, Jiang H, Peng B, Bian Z (2010) Effect of bioaggregate on differentiation of human periodontal ligament fibroblasts. *International Endodontic Journal* **43**, 1116–21.

Yuan Z, Peng B, Jiang H, Bian Z, Yan P (2010) Effect of bioaggregate on mineral-associated gene expression in osteoblast cells. *Journal of Endodontics* **36**, 1145–8.

Zhang H, Pappen FG, Haapasalo M (2009) Dentin enhances the antibacterial effect of mineral trioxide aggregate and bioaggregate. *Journal of Endodontics* **35**, 221–4.